Realistic microscopic level densities for spherical nuclei

Nicolas Cerf
Division de Physique Théorique, Institut de Physique Nucléaire, Orsay Cedex 91406, France
(Received 30 March 1994)

Nuclear level densities play an important role in nuclear reactions such as the formation of the compound nucleus. We develop a microscopic calculation of the level density based on a combinatorial evaluation from a realistic single-particle level scheme. This calculation makes use of a fast Monte Carlo algorithm allowing us to consider large shell model spaces which could not be treated previously in combinatorial approaches. Since our model relies on a microscopic basis, it can be applied to exotic nuclei with more confidence than the commonly used semiphenomenological formulas. An exhaustive comparison of our predicted neutron s-wave resonance spacings with experimental data for a wide range of nuclei is presented.

PACS number(s): 21.10.Ma, 21.60.Ka, 02.70.−c

I. INTRODUCTION

Nuclear level densities for application to the calculation of nuclear reactions are traditionally described in the framework of the Fermi-gas statistical model [1–3]. Experimental data (especially on neutron resonances) provide a considerable amount of information on level densities, shedding some light on various failures of the statistical model. For example, the experimental determination of the variation of temperature with excitation energy indicates that the apparent level density parameter a depends on the excitation energy [4–6]. Also, some accurate measurements give evidence of a strong parity dependence of the level density at excitation energies around the neutron binding energy [7,8], in contrast with the classical assumption of parity equipartition [1]. As a matter of fact, many uncertainties still remain in the level density global parametrization systematics, due to the fact that most of the experimental knowledge is confined to narrow regions of excitation energy and angular momentum (see, e.g., [9]). In that context, one is still limited to a semiempirical description of various effects such as the shell corrections (especially, the thermal damping of shell effects) [9–12], the collective enhancement (rotational and vibrational increase) [13–15], the evolution of the spin distribution (spin cutoff parameter), or the pairing correlations [16].

In a previous paper [17], we have shown how a Monte Carlo method can be used to provide a computationally fast estimate of the level density that reproduces very closely the microscopic combinatorial evaluation for heavy nuclei and/or at high excitation energy, when a direct counting is impracticable. In this paper, we compute the combinatorial level densities of a wide range of nuclei by means of this Monte Carlo algorithm. We show that our microscopic calculation of the level density based on a realistic (Hartree-Fock with a Skyrme force) single-particle level scheme is an alternative to the current statistical estimates. With the Monte Carlo sampling procedure, we are able to consider large shell model spaces which could not be previously treated in combinatorial approaches. This model reliably accounts for shell and pairing effects. Moreover, since it relies on a microscopic foundation, it can be applied to exotic nuclei with more confidence than the commonly used semiphenomenological formulas. In this paper, we restrict ourselves to the case of spherical nuclei, but the method could be extended to deformed nuclei.

In Sec. II, we first outline the basis of the Monte Carlo method for calculating microscopic level densities and present some illustrative results. This method exhibits various failures of the statistical model such as the problem of the spin-parity distribution or the thermal damping of shell effects. An exhaustive comparison of our predicted neutron s-wave resonance spacings with the available experimental data for a large set of nuclei is then presented in Sec. III. The evidence of a collective enhancement of level densities is discussed in the light of this comparison. Finally, we conclude in Sec. IV.

II. MICROSCOPIC LEVEL DENSITIES

The statistical model of nuclear reactions traditionally makes use of a statistical description of the nuclear level density (e.g., the back-shifted Fermi-gas model [18–21]), although such a description is known to provide an approximate estimate which does not describe very reliably shell and pairing effects. Alternatively, a microscopic combinatorial determination of the level density (see, e.g., [22–24]) based on an exhaustive counting of the excited levels can be considered, but it is known to require an exceedingly long computation time, especially for large nuclear mass number A. This is the reason why this method is often dismissed. However, we have shown in a previous work [17,25] that a Monte Carlo technique can be used to avoid this direct counting procedure, and makes thus possible a fast microscopic calculation of level densities. Indeed, it is well known that Monte Carlo methods generally provide very efficient algorithms for solving combinatorial problems. Moreover,

 ©1994 The American Physical Society

a direct counting procedure cannot easily treat the residual interaction in nuclei because it is then prohibitively time consuming, so that it is natural to resort to a Monte Carlo technique.

A. Monte Carlo method

The Monte Carlo simulation makes use of the Metropolis sampling scheme [26], which has been widely applied in statistical mechanics (see, e.g., [27,28]). It is based on a random sampling of a very small fraction of the excited levels in the range of excitation energy under consideration [17,25]. The resulting sample is assumed to be representative of the whole configuration space, analogous with what is done when estimating a multidimensional integral by a Monte Carlo procedure (see, e.g., [27]). Thus, the properties of the whole spectrum of excited states (i.e., energy, spin, parity, or other quantities) can be simply derived by extrapolating from the sample and applying the appropriate scale factor. Of course, although the method is asymptotically exact, the resulting level density is inherently affected by a statistical error scaling as $N^{-1/2}$, where N is the size of the sample. However, this means that the accuracy can be imposed by choosing an appropriate size N for the sample, and does not depend on the actual number of levels in the considered energy range. (For instance, a rough estimate may be obtained within a very short computation time by sampling only a few configurations.) The Metropolis sampling scheme consists in following a guided random walk which proceeds through configuration space (see [17]). At each step, a new (trial) configuration is chosen at random according to a given distribution, and this (trial) move is either accepted or rejected with a given probability. The limit distribution of this random walk is adjusted to ensure a more or less equal accuracy in the whole considered energy interval (i.e., the configuration space is uniformly explored in energy). The reliability of this Monte Carlo procedure is ascertained by the fact that the computed total level density is in perfect agreement with a direct counting (when workable), as shown in [17]. The same conclusion holds for the spin and parity distributions of the excited levels.

This Monte Carlo method can also be easily extended in order to account for the pairing interaction in the standard BCS approximation at essentially no cpu cost. In analogy to what is done in combinatorial methods (see [22,24]), the total energy of each sampled (proton or neutron) configuration C is given by

$$E_C = \sum_k{}' \epsilon_k + \sum_k{}'' 2\epsilon_k v_{k,C}^2 - \Delta_C^2/G \ , \qquad (1)$$

where G is the pairing strength parameter, ϵ_k are the single-particle state energies, and $v_{k,C}^2$ are calculated from

$$v_{k,C}^2 = \frac{1}{2}\left\{1 - \frac{\epsilon_k - \lambda_C}{[(\epsilon_k - \lambda_C)^2 + \Delta_C^2]^{1/2}}\right\} \ , \qquad (2)$$

Δ_C and λ_C being obtained by solving the pair of BCS equations

$$\sum_k{}'' 2v_{k,C}^2 = \eta_C \ , \qquad (3)$$

$$\sum_k{}'' [(\epsilon_k - \lambda_C)^2 + \Delta_C^2]^{-1/2} = 2/G \ . \qquad (4)$$

Here, Δ_C and λ_C are the gap parameter and Fermi energy, respectively, while η_C stands for the number of paired nucleons. Following the notation of Ref. [22], the summation $\sum'$ is made over orbitals containing unpaired nucleons, while $\sum''$ is made over orbital pairs in which there is not an unpaired nucleon. Thus, we use the so-called blocking method [22,29], that is the orbits occupied by unpaired nucleons are blocked (i.e., unavailable for pair diffusion). More precisely, we restrict ourselves to an approximate inclusion of pairing, close to what is done in Ref. [24], where the excitations involving promoted pairs are neglected. All the excited particles are thus taken as noninteracting excitons, and the orbitals in which they are placed are excluded from the BCS consideration even if two particles occupy time-reversed orbitals. This approximation can be justified by arguing that the number of such configurations involving promoted pairs is very small (see [17]). When the excitation energy increases, more and more orbital pairs are blocked, so that only the trivial solution $\Delta = 0$ can exist, in general, above a certain energy. This behavior is in qualitative agreement with the result of the temperature-dependent BCS theory [30]. The investigation of the level density problem including the pairing force via a Monte Carlo procedure is the subject of a future work.

Note that the inclusion of BCS equations in a combinatorial computation is well known to be generally exceedingly time consuming, so that the Monte Carlo approach becomes invaluable in that case. Indeed, we have found that the additional amount of cpu time needed for the inclusion of pairing in our Monte Carlo procedure is only about 30–40 %, even if the BCS equations are solved repeatedly (for each sampled configuration). This surprisingly small increase originates from the fact that only about 1% of the Metropolis (trial) moves are accepted on average along our random walk, so that the extra cpu time needed to compute the pairing energy (by solving BCS equations) only concerns about 1% of the configurations. Accordingly, the energy of the remaining (99%) configurations does not need to be calculated, allowing a significant gain of computing time. The latter configurations are necessary, however, to associate the appropriate statistical weights to the former 1% configurations that are actually sampled.

B. Comparison with a Fermi-gas model

In order to illustrate the accuracy gained by using the microscopic Monte Carlo calculation, we compare our results with the predictions of a Fermi-gas statistical model. In the following, we consider a traditional level density model which is based on the conventional meth-

ods of statistical mechanics [3]. The total state density $\omega(U)$ for a two-components system as a function of the excitation energy U is expressed by

$$\omega(U) = \frac{\exp[S(U)]}{(2\pi)^{3/2} D(U)^{1/2}} , \tag{5}$$

where $S(U)$ denotes the entropy and $D(U)$ is the determinant related to the saddle-point approximation. For the Fermi-gas model, assuming equidistant single-particle states with a density g (for both neutrons and protons) and an empirical shift Δ (accounting for pairing and shell corrections), the following relations hold:

$$a = \frac{\pi^2}{6} g , \tag{6}$$

$$U - \Delta = at^2 - t , \tag{7}$$

$$S(U) = 2\sqrt{(at)^2 - at} , \tag{8}$$

$$D(U) = \frac{18}{\pi^4} a^3 t^5 , \tag{9}$$

where t is the thermodynamic temperature (in the Lang and Le Couteur [31] definition). The resulting expression for the state density is

$$\omega(U) = \frac{\sqrt{\pi}}{12} \frac{\exp\left[2\sqrt{a(U-\Delta)}\right]}{a^{1/4}(U-\Delta+t)^{5/4}} . \tag{10}$$

Assuming a Gaussian distribution for the angular momentum projection, the corresponding expression for the total level density is clearly

$$\rho(U) = \frac{\omega(U)}{\sqrt{2\pi\sigma^2}} = \frac{1}{12\sqrt{2}} \frac{\exp\left[2\sqrt{a(U-\Delta)}\right]}{\sigma a^{1/4}(U-\Delta+t)^{5/4}} , \tag{11}$$

where σ^2 is the spin cutoff parameter. In the comparison, we use the values of the parameters a, Δ, and σ^2, tabulated for many nuclei from the compilation by Dilg *et al.* [20]. Note that those parameters slightly depend on the adopted value for the inertia moment of the nucleus (see Sec. II D), so that we consider in the following the range 50–100 % of the rigid-body value, as in Ref. [20].

Concerning the microscopic Monte Carlo calculation, we use the spherical single-particle level scheme resulting from a Hartree-Fock + BCS calculation based on a Skyrme interaction from Ref. [32]. In order to be consistent, we solve the BCS equations for all the excited configurations with the values for the pairing strength parameters $G_n = 2.25/N^{0.7}$ MeV (for neutrons) and $G_p = 2.00/Z^{0.7}$ MeV (for protons) derived in Ref. [32] for the ground state. For illustrative purposes, we consider the cases of 5 nuclei, ^{88}Sr, ^{102}Ru, ^{140}La, ^{166}Ho, and ^{196}Pt. In Fig. 1, we plot the total level density $\rho(U)$ versus excitation energy U. The solid histogram represents the microscopic Monte Carlo calculation, while the dotted and the dashed lines show the statistical predictions from Ref. [20] with a moment of inertia equal to 50% and 100% of the rigid-body value, respectively. Note that a basis of spherical single-particle states is used here for all nuclei, even if it is clearly not a realistic choice especially for ^{166}Ho. Moreover, we ignore the enhancement factor due to the contribution of rotational bands in this deformed nucleus [14]. However, our purpose is simply to compare our Monte Carlo method with a simple statistical model, and to exhibit the discrepancies. Notice that the total number of states up to 30 MeV for a heavy odd-odd nucleus such as ^{166}Ho becomes as high as $\sim 10^{18}$, a number obviously out of reach of any combinatorial procedure. One could *a priori* think that, with such a number of excited levels, the conventional statistical model would be sufficiently accurate (one has rapidly entered into the statistical regime), but it appears that this is not necessarily the case.

In particular, it is clear that the parameter a cannot be considered as a constant, as it is assumed in the traditional statistical method (e.g., the back-shifted Fermi gas model [20]). This discrepancy is well known to be a consequence of shell effects (see, e.g., [10–12]). Ignatyuk *et al.* [10] have noted that calculations based on realistic single-particle states predict shell effects in the level density which may be pronounced at low excitation energy and tend to disappear only at higher energies. They proposed a simple semiempirical model which accounts for such energy-dependent shell effects by relating them to the ground-state shell correction $E_{\rm shell} = M_{\rm exp} - M_{\rm drop}$, defined as the difference between the experimental mass $M_{\rm exp}$ and the liquid drop mass $M_{\rm drop}$ [33]. In this model, they introduce an energy-dependent parameter a defined by

$$a(U) = \tilde{a}\left[1 + E_{\rm shell}\frac{1-\exp(-\gamma U)}{U}\right] , \tag{12}$$

where $\tilde{a}$ is the asymptotic a parameter which should exhibit no shell effects, and γ is a free parameter determined by comparison with calculations using realistic single-particle states. Given the fact that $E_{\rm shell}$ is negative for a nucleus close to a shell closure, the a parameter for, e.g., ^{88}Sr, ^{140}La, and ^{196}Pt should monotonically increase up to its asymptotic value, as confirmed qualitatively by Figs. 1(a), (c), and (e). On the contrary, for a nucleus far from shell closure ($E_{\rm shell} > 0$), the a parameter should be a decreasing function of U. However, this behavior does not appear in Figs. 1(b) and 1(d), showing that the microscopic $a(U)$ is certainly more complex than predicted by Eq. (12). The case of ^{166}Ho exhibits a particularly bad agreement, but this may be due to our choice of a clearly unrealistic single-particle spectrum. Kataria *et al.* [11] have established another model to account for shell effects, based on a Fourier expansion of the shell fluctuations of the single-particle state density. This model is however closely related to the Ignatyuk *et al.* model. More recently, Goriely [34] has proposed a more microscopic model which uses a semiclassical approximation to the single-particle state density to describe the influence of the nuclear shell structure on the energy dependence as well as on the spin distribution of the level density. This model yields an analytical approximation to the spin-dependent level density, obtained in the framework of a microscopic statistical model. However, this model leaves

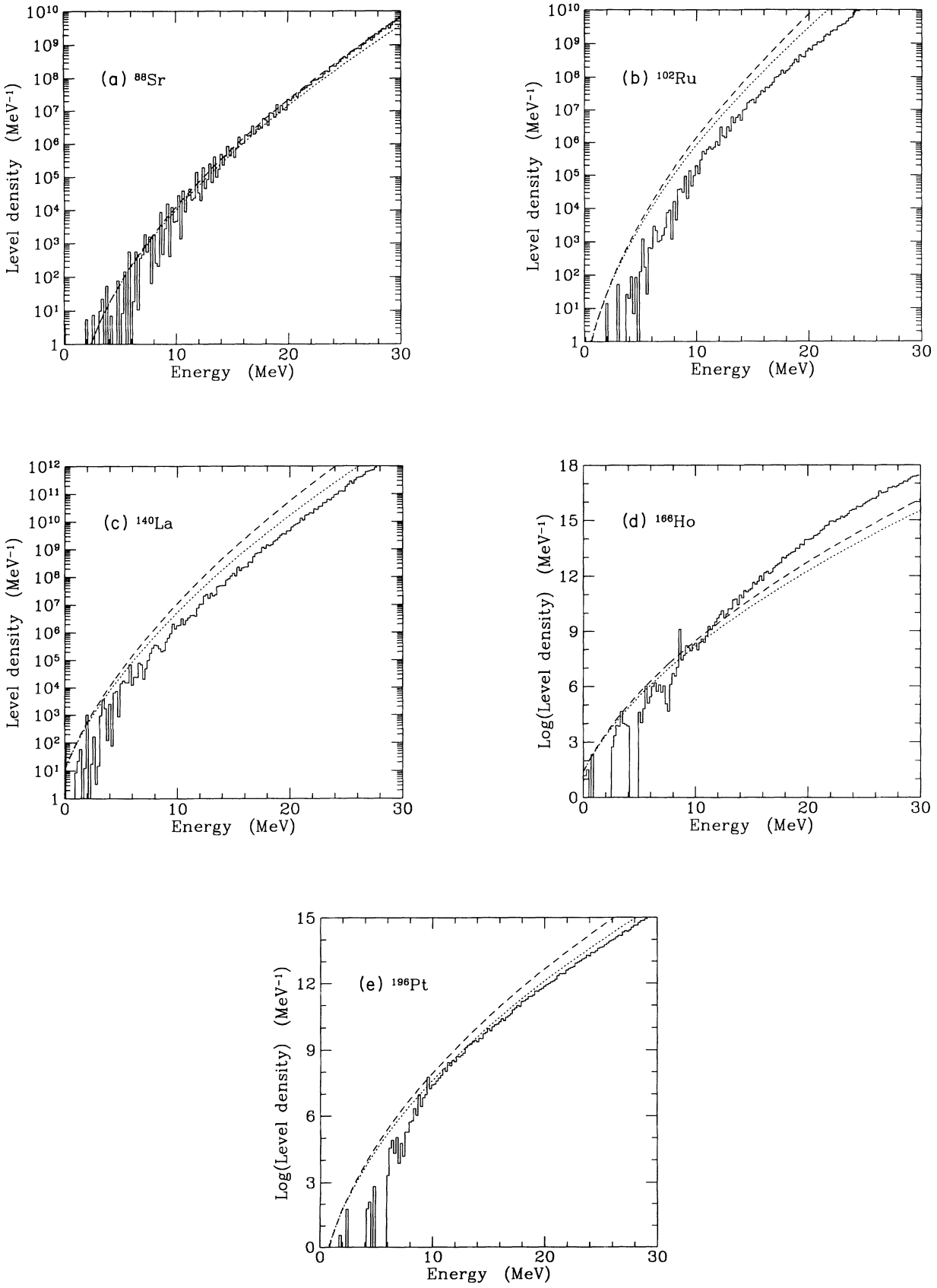

FIG. 1. Total level density $\rho(U)$ vs excitation energy U for (a) ^{88}Sr, (b) ^{102}Ru, (c) ^{140}La, (d) ^{166}Ho, and (e) ^{196}Pt. The solid histogram represents the microscopic Monte Carlo calculation, while the dotted and the dashed lines show the statistical predictions from Ref. [20] with a moment of inertia equal to 50% and 100% of the rigid-body value, respectively.

undetermined some free parameters that need to be fixed by recoursing to realistic calculations. In this respect, the Monte Carlo method proves to be very useful because it allows to check a semiphenomenological formula by a comparison with exact counting results, especially in the asymptotic region.

C. Spin-parity distribution

Let us turn now to the spin-parity dependence of the level density. In the conventional statistical model, the dependence of the state density upon the angular momentum projection M has the Gaussian form [1,3]

$$\omega(U,M) = \omega(U)\frac{\exp(-M^2/2\sigma^2)}{\sqrt{2\pi\sigma^2}} , \qquad (13)$$

where σ^2 is the spin cutoff parameter, and $\omega(U)$ stands for the total state density [Eq. (5)]. The resulting spin-dependent level density can be written as

$$\rho(U,J) \simeq -\left[\frac{\mathrm{d}}{\mathrm{d}M}\,\omega(U,M)\right]_{M=J+1/2} \simeq \frac{2J+1}{2(2\pi)^{1/2}\sigma^3}\exp\left[-\frac{(J+1/2)^2}{2\sigma^2}\right]\omega(U) , \qquad (14)$$

where J denotes the total angular momentum of the levels at excitation energy U. Concerning the parity dependence, the statistical model predicts that both parities contribute in equal amounts to the level density (see [1]).

In Fig. 2, we plot the spin distribution (for each parity) of the levels of ^{142}Pr in the energy interval [5.8–6.0 MeV] around the neutron separation energy. Given the odd-odd character of ^{142}Pr, the number of excited levels in this energy interval is as high as 1.7×10^4. Therefore, the spin distribution calculated by the Monte Carlo method is expected to be consistent with the asymptotic distribution of the statistical model. In order to check that, we estimate an effective spin cutoff parameter σ^2 by calculating the variance of the Monte Carlo derived M distribution. This yields the value $\sigma^2 \simeq 28.8$, corresponding to a maximum in the J distribution at a spin around $\sigma \simeq 5$. The corresponding spin distribution with this adopted value for σ^2 is also plotted in Fig. 2. The agreement with the microscopic calculation is evident. It illustrates that one can be confident in the asymptotic result if one is concerned with an energy interval containing a sufficiently large number of levels (and provided that σ^2 is sufficiently well known). Note that, in spite of this large number of levels, the parity equipartition is not achieved yet in the considered energy interval, illustrating the need for an appropriate treatment of parity (see [35]).

In Fig. 3, we consider the spin distribution of ^{208}Pb in the energy interval [7.3–8.0 MeV] situated just above the neutron separation energy. That interval corresponds to the one used by Dilg *et al.* [20] in their analysis of experimental average neutron s-wave resonance spacings. The number of levels belonging to that interval is estimated to be about 100 (see [25]), so that statistical results are expected to be unreliable. This is indeed what appears

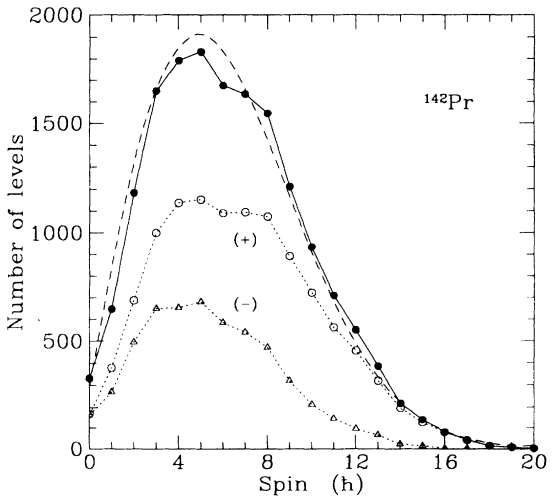

FIG. 2. Spin distribution of the excited levels for ^{142}Pr in the energy interval [5.8–6.0 MeV] resulting from our Monte Carlo calculation. The solid circles represent the total (with both parities) distribution, while the positive- and negative-parity distributions are represented by open circles and triangles, respectively. The dashed line shows the asymptotic distribution from the statistical model [Eq. (14)]. The derived value for the effective spin cutoff parameter is $\sigma^2 \simeq 28.8$.

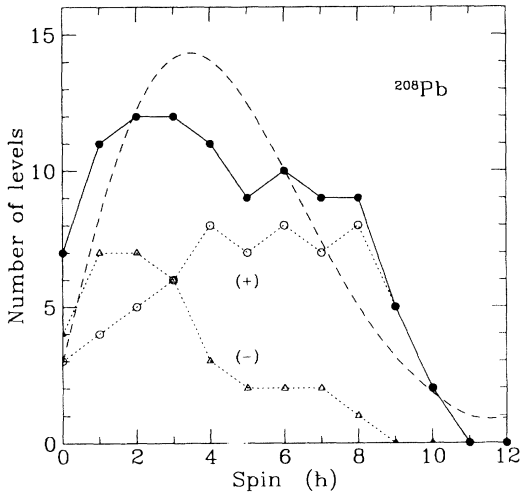

FIG. 3. Spin distribution of the excited levels for ^{208}Pb in the energy interval [7.3–8.0 MeV]. The solid line corresponds to $\rho(U,J)$ resulting from our Monte Carlo calculation, while the dashed line represents the asymptotic distribution from the statistical model [Eq. (14)]. The derived value for the effective spin cutoff parameter is $\sigma^2 \simeq 15.5$. The solid circles represent the total (with both parities) Monte Carlo distribution, while the positive- and negative-parity distributions are represented by open circles and triangles, respectively. Note that, for consistence, the number of levels of each spin provided by the Monte Carlo simulation for ^{208}Pb has been rounded to the nearest integer.

in Fig. 3 where we compare the Monte Carlo derived spin distribution with the asymptotic result [Eq. (14)]. The spin cutoff parameter is found to be $\sigma^2 \simeq 15.5$. Even with this "best-fitted" value of σ^2, the spin distribution is badly reproduced by the statistical model. In particular, this model very poorly predicts the number of low-spin levels ($J = 0, 1$) that are generally needed to compare the experimental neutron s-wave spacings with theory (see Sec. III). Therefore, one should be very careful when attempting to extrapolate total level densities from the experimental densities of levels at given spin(s). Since the compilations of experimental nuclear level densities (see [12,20], or the recent Ref. [9]) always assume the validity of the statistical spin distribution, that extrapolation is a source of uncertainties. The same remark applies to the parity equipartition commonly assumed in all the compilations.

D. Spin cutoff parameter

Equally important is the evolution of the spin cutoff with excitation energy. In the traditional Fermi gas model assuming equidistant single-particle states with a density g, the spin cutoff is related to the temperature t by

$$\sigma^2(U) = g\langle m^2 \rangle t \ , \tag{15}$$

where $\langle m^2 \rangle$ is the average value of the squared angular momentum projection of the single-particle states at the Fermi energy. From theoretical arguments [1], σ^2 is expected to approach at high excitation the value

$$\sigma^2_{\rm rigid} = \frac{1}{\hbar^2}\Theta_{\rm rigid}\ t \approx 0.0150 A^{5/3}\ t \ , \tag{16}$$

where $\Theta_{\rm rigid} = \frac{2}{5}MR^2$ is the rigid body moment of inertia, and a nuclear radius $R \approx 1.25A^{1/3}$ fm is assumed. However, experimental data [20] indicate that values between 50% and 100% of the rigid-body value are preferable, so that one writes

$$\sigma^2 = \frac{1}{\hbar^2}\Theta_{\rm eff}\ t, \tag{17}$$

where $\Theta_{\rm eff}$ can be regarded as an effective moment of inertia of the nucleus under consideration, and is usually chosen between $\frac{1}{2}\Theta_{\rm rigid}$ and $\Theta_{\rm rigid}$ (see [20]).

In contrast with such a simple description, our calculations for ^{208}Pb indicate that the spin cutoff parameter exhibits shell effects [36]. In Fig. 4, we show the evolution of the spin cutoff parameter for ^{208}Pb as a function of excitation energy U. As it asymptotically occurs like $\sigma^2 \sim \sqrt{U}$, we rather plot the quantity $\sigma^2/\sqrt{U}$ which should asymptotically behave like a constant (according to the statistical model predictions). The solid line represents the result of the Monte Carlo method (each point corresponding to a Monte Carlo simulation), while both dashed lines stand for the prediction of the statistical model with $\Theta_{\rm eff} = \frac{1}{2}\Theta_{\rm rigid}$ and $\Theta_{\rm rigid}$. In that calculation, we took the values for a and Δ from the compilation by

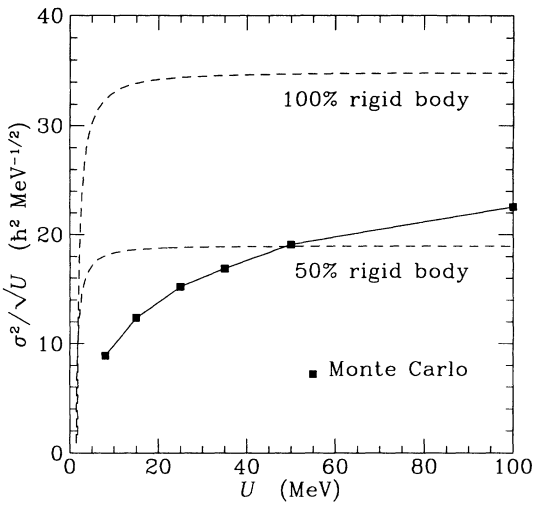

FIG. 4. Evolution of $\sigma^2/\sqrt{U}$ as a function of excitation energy U for ^{208}Pb, with σ^2 denoting the spin cut-off parameter. The solid line represents the result of our Monte Carlo method (each point corresponding to a Monte Carlo simulation), while both dashed lines stand for the prediction of the statistical model [20] with a moment of inertia equal to 50% and 100% of the rigid-body value, respectively. We took $a = 8.53$ MeV^{-1}, $\Delta = 1.52$ MeV for the 50% case, and $a = 10.02$ MeV^{-1}, $\Delta = 1.80$ MeV for the 100% case, as in Ref. [20].

Dilg *et al.* [20]. Note that, in order to check the asymptotic behavior, we had to go to an excitation energy as high as 100 MeV, which is possible only with the Monte Carlo method. The $\sigma^2/\sqrt{U}$ curve is another evidence of shell effects: for this doubly magic nucleus, the $\sigma^2/\sqrt{U}$ slowly increases towards its asymptotic value (which is compatible with the predicted value from the traditional statistical model). Thus, the spin cutoff is clearly overestimated in that model, at least in an intermediate energy range (around the neutron separation energy). One should observe the opposite behavior for nuclei far from shell closures. Note that, as far as spin distribution is concerned, the Monte Carlo method is the only method able to provide a realistic—microscopically calculated—spin cutoff in a broad energy range, up to high excitation energies. (It gives the spin cutoff that an exact counting would have provided, if feasible.) Therefore, it could also be useful to predict parameters of semiphenomenological formulas for the spin distribution.

III. COMPARISON WITH EXPERIMENTAL DATA

Neutron resonance data constitute the most detailed source of knowledge concerning the level density of highly excited nuclei. A large body of experimental data about neutron resonances is currently available, and we have carried out a systematic confrontation of our results with the neutron resonance spacings from the most recent compilation by Iljinov *et al.* [9].

The excited levels that are revealed by neutron resonance spectroscopy have narrowly selected values of angular momentum and parity quantum numbers. In particular, the resonances which are excited by s-wave neutrons (i.e., those which are expected to have a much greater strength than other resonances) are those with a spin $|J_t \pm 1/2|$ and a parity π_t, where J_t and π_t are the ground state spin and parity of the target nucleus, respectively. Thus, the neutron resonance experiments yield the number of s-wave resonances having the appropriate spin and parity within a given interval around the neutron separation energy S_n, from which the average spacing D is deduced. In this section, we compare the experimental values of the s-wave resonance spacings at neutron separation energy taken from [9], $D_{\rm exp}$, with the spacings derived from the Monte Carlo calculation, $D_{\rm MC}$ (see also [36]). Note that this direct comparison of D is preferable to what is done in the compilations of experimental nuclear level densities, which assume the validity of the statistical spin distribution along with the parity equipartition. Indeed, the usual procedure (see, e.g., [2]) that provides the level density parameter a from experiments is to write the level density of the observed s-wave resonances as

$$\frac{1}{D_{\rm exp}} = \frac{1}{2} \sum_{J=|J_t-1/2|}^{|J_t+1/2|} \rho_{\rm exp}(S_n, J), \tag{18}$$

that is as a summation over observable spins, where

$$\rho_{\rm exp}(U, J) = \rho_{\rm exp}(U) \frac{2J+1}{2\sigma^2} \exp\left(-\frac{(J+\frac{1}{2})^2}{2\sigma^2}\right) . \tag{19}$$

The value of a is obtained by a fit of $\rho_{\rm exp}(U)$ with a Fermi-gas expression such as Eq. (11). This procedure has to be used with care since (i) it involves the assumption that the spins are distributed according to the statistical distribution; (ii) the spin cutoff factor is unknown experimentally; and (iii) the factor 1/2 in Eq. (18) holds only if both parities are equidistributed. The assumptions (i) and (iii) are clearly not valid in some cases, and (ii) is a source of uncertainties, as shown in Secs. II C and II D.

Figure 5 shows the experimental [9] spacing $D_{\rm exp}$ as a function of the mass number A for about 200 nuclei along the stability valley (with $20 \leq A \leq 208$). The most represented nuclei in this set are even Z-odd N (solid circles), since they come from experiments on even-even targets. There is almost the same number of even-even (open circles) and odd-odd (open triangles) nuclei, corresponding both to odd-A targets, while there are only a few data concerning odd Z-even N nuclei (crosses) since they come from experiments on odd-odd targets. Shell and even-odd effects are clearly visible in Fig. 5. The odd-A nuclei (which are essentially even Z-odd N) are systematically shifted to larger spacings than their even-even neighbor nuclei, as a consequence of the lower neutron separation energy S_n for odd neutron number nuclei. For the odd-odd nuclei, however, this effect is counterbalanced by a lower pairing shift which tends to increase the level density, thus decreasing the average spacing.

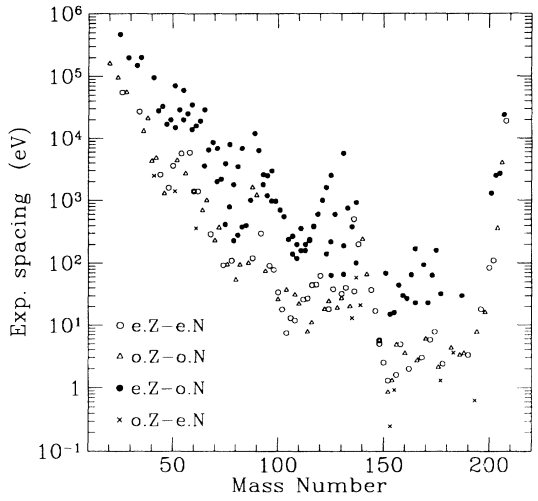

FIG. 5. Experimental spacing $D_{\rm exp}$ from [9] as a function of the mass number A for about 200 stable nuclei. The even-even and odd-odd nuclei are represented by open circles and triangles, respectively, while the even Z-odd N and odd Z-even N nuclei correspond to solid circles and crosses, respectively.

Figure 6 shows the ratio $R = D_{\rm MC}/D_{\rm exp}$ for the same set of nuclei, $D_{\rm MC}$ being averaged into a 900 keV interval around the neutron separation energy S_n in order to suppress small-scale oscillations in the level density [17].

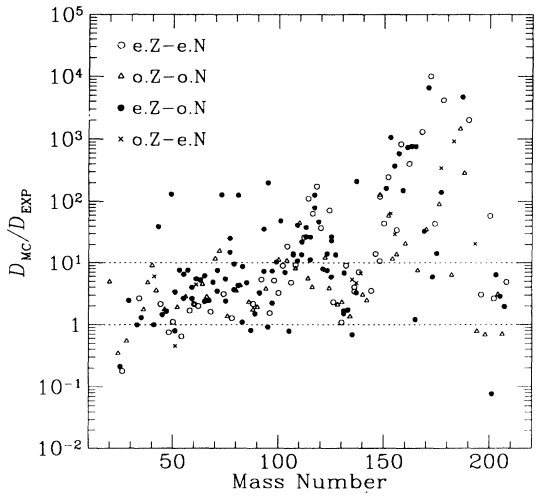

FIG. 6. Ratio R of the Monte Carlo to experimental [9] spacing as a function of the mass number A for about 200 stable nuclei. The Monte Carlo spacing is averaged into a 900 keV interval around the neutron separation energy. The even-even and odd-odd nuclei are represented by open circles and triangles, respectively, while the even Z-odd N and odd Z-even N nuclei correspond to solid circles and crosses, respectively. The region with $1 \leq R \leq 10$ is delimited by dotted lines.

Note that, for a very small number of nuclei, the Monte Carlo calculation provides a zero level density in this interval, so that these nuclei were excluded from the comparison. Such a comparison of experimental data with a combinatorial-like calculation for a large sample of nuclei is only possible thanks to the Monte Carlo method. The conclusions of this comparison are the following. First, the even–odd effects visible in Fig. 5 have vanished, suggesting that pairing has been reasonably taken into account. Second, it is clear that the overall fluctuation of R is satisfactory, given the fact that $D_{\rm exp}$ spans more than six decades. In fact, the ratio R is found to lie between 1 and 10 for a large amount of the nuclei. The regions where this ratio exceeds about 10 correspond clearly to regions of nuclear deformation. This is understandable since our model in its present state of development relies on a spherical single-particle spectrum and does not account for the rotational enhancement factor. Indeed, realistic calculations of the collective (vibrational or rotational) enhancement of level densities based on the interacting boson model [37,38] suggest that the magnitude of this effect typically lies between 10 and 100. Moreover, Fig. 6 shows evidence for neutron shell effects: the ratio R exhibits dips at $A \sim 50$, 90, 140, and 210, corresponding approximately to the neutron shell closures at $N =$ 28, 50, 82, and 126. Finally, the weak systematic bias (the averaged ratio being larger than unity) might be related to the fact that practically all nuclei have a nonzero equilibrium deformation in the ground state, suggesting a collective enhancement of the level density in general (see [9] and reference therein). Figure 7 represents the same data in the $N - Z$ plane. The regions of nuclear deformation (especially the rare earth region) appear clearly.

In order to give a quantitative estimate of the quality of the overall agreement between the Monte Carlo calculation and experimental data, we use the so-called f factor (see [2,9,39]) measuring the dispersion of the ratios, and defined as the rms value

$$f \equiv \exp\sqrt{\langle \ln^2 R \rangle} \qquad (20)$$

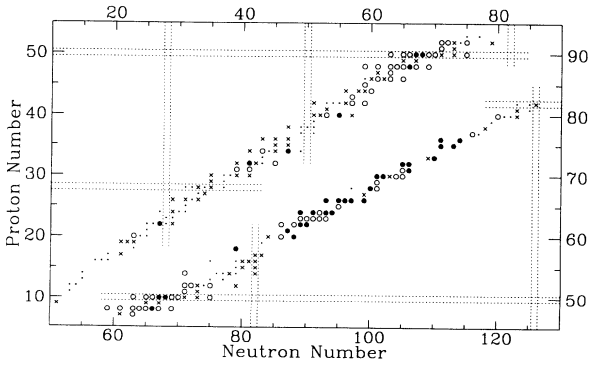

FIG. 7. Ratio R of the Monte Carlo to experimental spacing in the $N - Z$ plane. The symbols represent the following values: $R < 3$ (dots), $3 < R < 10$ (crosses), $10 < R < 100$ (open circles), and $R > 100$ (solid circles). The magic proton and neutron numbers are represented by dotted lines.

TABLE I. Average ratio $\bar{R}$ and (rescaled) f factor for the whole set of nuclei, and separately for each class of nuclei. Note that the highly deformed nuclei in the range $150 \leq A \leq 190$ are omitted here. The second column gives the number of nuclei in each class, along with the total number of nuclei (between parentheses) including those deformed nuclei.

	Number	$\bar{R}$	f
All classes	169 (208)	5.3	4.3
Even Z-even N	41 (51)	5.5	4.7
Odd Z-odd N	40 (50)	3.4	3.1
Even Z-odd N	81 (96)	6.5	4.6
Odd Z-even N	7 (11)	4.6	2.9

where the symbol $\langle\,\rangle$ stands for an average over the experimental points. Not considering the highly deformed rare earth nuclei in this comparison, the resulting f factor (after rescaling the ratios) has a value of about 4. (This means that the Monte Carlo method predicts the level density within a factor of about 4.) This value has to be compared with the corresponding value $f \simeq 2$ for the phenomenological systematics of Ref. [9]. The higher quality of the latter approach is expected, as it results from fit to stable nuclei. In contrast, our computed level density has a microscopic basis (it is obtained from a realistic single-particle level scheme), and does not involve any fit to the experimental level density. We thus think that it is more reliable for exotic nuclei than the semiphenomenological formulas of common use in reaction rate calculations. The value of the (rescaled) f factor along with the average ratio

$$\bar{R} \equiv \exp\langle \ln R \rangle \qquad (21)$$

for the different classes of nuclei (omitting the nuclei in the range $150 \leq A \leq 190$) is summarized in Table I, illustrating the absence of any significant residual even-odd effect.

IV. CONCLUSION

The nuclear level density is a quantity of fundamental importance in nuclear reactions such as the formation of the compound nucleus. However, most current estimates of level densities for application to the calculation of nuclear reactions are based on the Fermi-gas statistical model. We present an alternative technique for estimating level densities on a more microscopic foundation, based on a Monte Carlo algorithm. This method provides a very accurate combinatorial estimate of the level density, namely when a direct counting is intractable. Our Monte Carlo determination sheds light on some inadequacies of the statistical model (e.g., the failure to predict a correct spin-parity distribution, or to describe reliably shell effects). The direct confrontation of our microscopically derived neutron s-wave resonance spacings with the available experimental data for a large body of nuclei also presents evidence for a collective enhance-

ment of level densities. This comparison is unique in that it does not rely on the traditionally used statistical assumptions. One really calculates the density of the levels with the observed spins and parities. It must be stressed that the discrepancies between both statistical and microscopic methods could be significant when calculating nuclear reaction cross sections. Also, since our computed level density is obtained from a microscopic basis—i.e., from a realistic single-particle level scheme—we think that it can be used for exotic nuclei with more confidence than the semiphenomenological formulas of common use in nuclear reaction calculations.

ACKNOWLEDGMENTS

We are grateful to E. De Sanctis for communicating to us experimental data on neutron resonances. We also express our gratitude to F. Tondeur and S. Goriely for providing us with helpful results. Finally, we thank M. Arnould, M. Rayet, and J. Vanhorenbeeck for useful discussions. The author is supported by a grant from the Human Capital and Mobility Program of the Commission of the European Communities. The Division de Physique Théorique is Unité de Recherche des Universités Paris XI et Paris VI associée au C.N.R.S.

[1] T. Ericson, Adv. Phys. **9**, 425 (1960).
[2] A. Gilbert and A. G. W. Cameron, Can. J. Phys. **43**, 1446 (1965).
[3] J. R. Huizenga and L. G. Moretto, Annu. Rev. Nucl. Sci. **22**, 427 (1972).
[4] G. Nebbia *et al.*, Phys. Lett. B **176**, 20 (1986).
[5] K. Hagel *et al.*, Nucl. Phys. **A486**, 429 (1988).
[6] M. Gonin *et al.*, Phys. Lett. B **217**, 406 (1989).
[7] D. J. Horen, J. A. Harvey, and N. W. Hill, Phys. Rev. C **20**, 478 (1979); **24**, 1961 (1981).
[8] H. M. Agrawal, J. B. Garg, and J. A. Harvey, Phys. Rev. C **30**, 1880 (1984).
[9] A. S. Iljinov *et al.*, Nucl. Phys. **A543**, 517 (1992).
[10] A. V. Ignatyuk, G. N. Smirenkin, and A. S. Tishin, Sov. J. Nucl. Phys. **21**, 255 (1975).
[11] K. Kataria, V. S. Ramamurthy, and S. S. Kapoor, Phys. Rev. C **18**, 549 (1978).
[12] H. Vonach, M. Uhl, B. Strohmaier, B. W. Smith, E. G. Bilpuch, and G. E. Mitchell, Phys. Rev. C **38**, 2541 (1988).
[13] A. V. Ignatyuk, K. K. Istekov, and G. N. Smirenkin, Sov. J. Nucl. Phys. **29**, 450 (1979).
[14] A. V. Ignatyuk, *The Statistical Properties of the Excited Atomic Nuclei* (Energoatomizdat, Moscow, 1983).
[15] A. I. Blokhin, A. V. Ignatyuk, and Y. N. Shubin, Sov. J. Nucl. Phys. **48** 232 (1988).
[16] A. Bohr and B. R. Mottelson, *Nuclear Structure* (Benjamin, New York, 1969).
[17] N. Cerf, Phys. Rev. C **49**, 852 (1994).
[18] E. Gadioli and L. Zetta, Phys. Rev. **167**, 1016 (1968).
[19] H. Vonach and M. Hille, Nucl. Phys. **A127**, 289 (1969).
[20] W. Dilg, W. Schantl, H. Vonach, and M. Uhl, Nucl. Phys. **A217**, 269 (1973).
[21] T. von Egidy, H. M. Schmidt, and A. N. Bekhami, Nucl. Phys. **A481**, 189 (1988).
[22] M. Hillman and J. R. Grover, Phys. Rev. **185**, 1303 (1969); M. Hillman, Phys. Rev. C **9**, 289 (1974).
[23] B. Pichon, Nucl. Phys. **A568**, 553 (1994).
[24] M. Herman and G. Reffo, Phys. Rev. C **36**, 1546 (1987); M. Herman, G. Reffo, and R. A. Rego, *ibid.* **37**, 797 (1988).
[25] N. Cerf, Phys. Lett. B **268**, 317 (1991).
[26] N. Metropolis, A. W. Rosenbluth, M. N. Rosenbluth, A. H. Teller, and E. Teller, J. Chem. Phys. **21**, 1087 (1953).
[27] J. M. Hammersley and D. C. Handscomb, *Monte Carlo Methods* (Methuen, London, 1964).
[28] K. Binder, in *Monte Carlo Methods in Statistical Physics*, edited by K. Binder (Springer-Verlag, New York, 1979).
[29] S. Wahlborn, Nucl. Phys. **37**, 554 (1962).
[30] P. Decowski, W. Grochulski, A. Marcinkowski, K. Siwek, and Z. Wilhelmi, Nucl. Phys. **A110**, 129 (1968).
[31] J. M. B. Lang and K. J. Le Couteur, Proc. Phys. Soc. A **67**, 585 (1954).
[32] F. Tondeur, Nucl. Phys. **A303**, 185 (1978); *ibid.* **A311**, 51 (1978); *ibid.* **A315**, 353 (1979).
[33] W. D. Meyers and W. S. Swiatecki, Ark. Fys. **36**, 343 (1967).
[34] S. Goriely, Ph.D. thesis, Oxford, 1991 (unpublished).
[35] N. Cerf, Nucl. Phys. **A554**, 85 (1993).
[36] N. Cerf, M. Rayet, and M. Arnould, in *Proceedings of the 8th International Symposium on Capture Gamma-Ray Spectroscopy and Related Topics*, edited by J. Kern (World Scientific, Singapore, 1994), p. 759.
[37] G. Maino, A. Mengoni, and A. Ventura, Phys. Rev. C **42**, 988 (1990).
[38] A. Mengoni and G. Maino, in *Proceedings of the 2nd International Symposium on Nuclear Astrophysics (Nuclei in the Cosmos)*, edited by F. Käppeler and K. Wisshak (Institute of Physics and Physical Society, London, 1993), p. 411.
[39] J. E. Lynn, *The Theory of Neutron Resonance Reactions* (Clarendon, Oxford, 1968).